Available online at www.sciencedirect.com
SCIENCE DIRECT®
Journal of Chromatography A, 1076 (2005) 103–109
JOURNAL OF CHROMATOGRAPHY A
www.elsevier.com/locate/chroma

Identification of the microsomal oxidation metabolites of rutaecarpine, a main active alkaloid of the medicinal herb *Evodia rutaecarpa*

Yune-Fang Ueng [a,d], Hsi-Jung Yu [b], Chang-Hsin Lee [b], Ching Peng [b], Woan-Ching Jan [c], Li-Kang Ho [c], Chieh-Fu Chen [c], Ming-Jaw Don [a,*]

[a] *National Research Institute of Chinese Medicine, 155-1 Li-Nong Street, Sec. 2, Taipei 112, Taiwan, ROC*
[b] *Department of Chemistry, Chinese Culture University, Taipei, Taiwan, ROC*
[c] *Department of Pharmacology, National Yang-Ming University, Taipei, Taiwan, ROC*
[d] *Graduate Institute of Medical Sciences, Taipei Medical University, Taiwan, ROC*

Received 19 January 2005; received in revised form 8 March 2005; accepted 6 April 2005

Abstract

Rutaecarpine is a quinazolinocarboline alkaloid of the medicinal herb *Evodia rutaecarpa* and shows a variety of pharmacological effects. Four oxidation metabolites of rutaecarpine were prepared from 3-methylcholanthrene-treated rat liver microsomes. These metabolites had an $[M+H]^+$ ion at *m/z* 304. The structures of metabolites were identified by comparison of their liquid chromatograms and mass, absorbance, and ^{1}H NMR spectra with those of synthetic standards. Rutaecarpine was metabolized by microsomal enzymes to form 3-, 10-, 11-, and 12-hydroxyrutaecarpine. The formation of 10-hydroxyrutaecarpine was highly induced by a cytochrome P450 1A inducer, 3-methylcholanthrene.

Keywords: Rutaecarpine; Hydroxyrutaecarpine; Cytochrome P450; Rat

1. Introduction

Evodia rutaecarpa (*Wu-Chu-Yu*) is a traditional Chinese medicine used for the treatment of gastrointestinal disorders and headache [1]. Rutaecarpine (Fig. 1) is a main quinazolinocarboline alkaloid isolated from *E. rutaecarpa* and shows a variety of pharmacological effects including antithrombotic and vasorelaxant effects [2]. Recently, Lee et al. [3] used LC–MS/MS analysis to show that rutaecarpine was metabolized to form monohydroxylated and dihydroxylated metabolites by untreated rat liver microsomes. However, the positions of hydroxyl groups were not clear.

Microsomal cytochrome P450 (CYP)-dependent monooxygenase is the main enzyme system catalyzing the oxidations of most drugs [4]. Our previous report demonstrated that rutaecarpine was a selective and potent inhibitor of mouse and human CYP1A2 in vitro, and caused an inductive effect on mouse hepatic CYP1A1/1A2 in vivo [5,6]. Rutaecarpine fits well in the active site of CYP1A2 [7]. 3-Methylcholanthrene is a typical inducer of CYP1A1 and CYP1A2 in rodents [8,9]. Thus, to identify the structures of rutaecarpine oxidation metabolites, rats were treated with 3-methylcholanthrene for metabolite isolation. In this report, our results demonstrated that rutaecarpine was metabolized by liver microsomal enzymes to form 3-, 10-, 11-, and 12-hydroxyrutaecarpine in untreated and 3-methylcholanthrene-treated rats. The formation of 10-hydroxyrutaecarpine was highly induced by 3-methylcholanthrene.

2. Experimental

2.1. Chemicals

Rutaecarpine and methoxyrutaecarpines were synthesized as described in previous report [7]. 1-, 2-, 3-, 4-, 9-, 10- , 11-, and 12-hydroxyrutaecarpine were synthesized from cor-

* Corresponding author. Tel.: +886 2 28201999x8411; fax: +886 2 2826 4266.
E-mail address: mjdon@nricm.edu.tw (M.-J. Don).

0021-9673/$ – see front matter © 2005 Elsevier B.V. All rights reserved.
doi:10.1016/j.chroma.2005.04.021

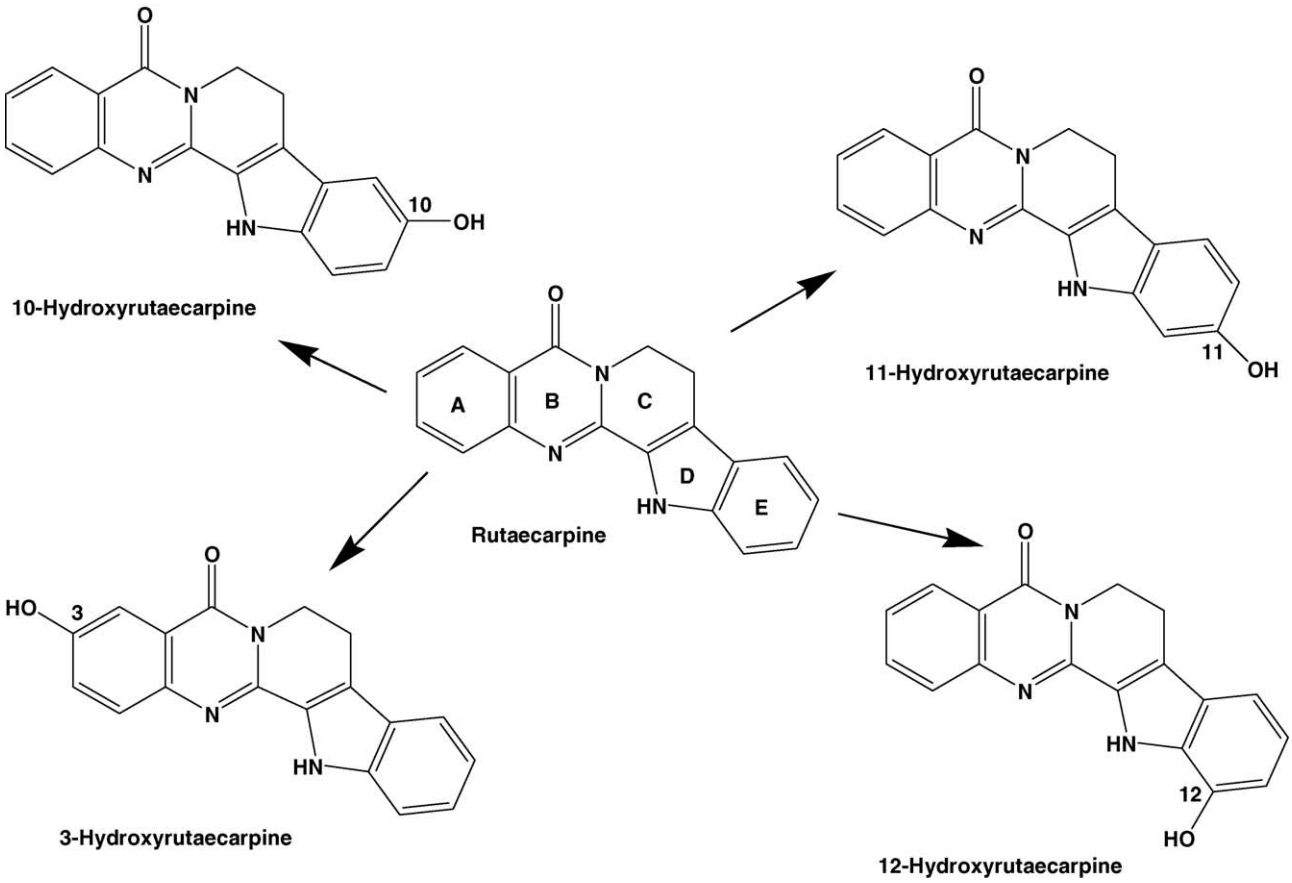

Fig. 1. Chemical structures of the main rutaecarpine oxidation metabolites in rat liver microsomes.

responding methoxyrutaecarpine by reaction with BBr_3 in dichloromethane or 1,2-dichloroethane under reflux [10]. The purities of rutaecarpine and hydroxyrutaecarpines were >98% as determined by HPLC and ^1H NMR analyses. Phosphoric acid, formic acid, and high-performance liquid chromatography (HPLC)-grade acetonitrile and methanol were purchased from Merck KGaA (Darmstadt, Germany). Glucose-6-phosphate, NADP, and glucose-6-phosphate dehydrogenase were purchased from Sigma-Chemico Inc. (St. Louis, MO, USA).

2.2. Animal treatment and microsomal preparation

Spraque–Dawley rats were purchased from National Yang-Ming University, Taipei. Rats were allowed a 1-week acclimation in the animal center with air conditioning ($25 \pm 2\,^{\circ}C$) and an automatically controlled photoperiod of 12 h light daily. All experimental protocols involving animals were reviewed and approved by the Institutional Animal Experimentation Committee of National Research Institute of Chinese Medicine. Rats were treated with 25 mg/kg/day 3-methylcholanthrene for 4 days. Liver microsomes were prepared by differential centrifugation at 4 °C [11]. Microsomal pellets were covered with 0.1 M potassium phosphate buffer, pH 7.4 and stored at −75 °C. Rutaecarpine oxidation assay was performed within 2 weeks.

2.3. Rutaecarpine oxidation assay and metabolite preparation

The microsomal reaction mixture consisted of 1 mg/ml microsomal protein, 200 μM rutaecarpine, 5 mM $MgCl_2$, and a NADPH-generating system in 50 mM potassium phosphate buffer, pH 7.4. The NADPH-generating system comprised 0.7 mM NADP, 13.7 mM glucose-6-phosphate, and 0.25 U/ml glucose-6-phosphate dehydrogenase. For analytical purpose, the incubation of 1.0 ml final volume was performed in 16 mm × 100 mm test tube without cap in a water bath at 37 °C for 20 min with shaking. After incubation, 50 μl 43% phosphoric acid was added to stop reaction. Oxidation products were extracted by 2 ml dichloromethane. One millilitre of the organic layer was dried under nitrogen and then dissolved in acetonitrile. Metabolites were separated by HPLC using a C18 column (Zorbax 4.6 mm × 250 mm, Agilent Technologies Inc., DE, USA) and eluted by a mobile phase containing 26% acetonitrile, 10% methanol, and 0.04% formic acid at 0–35 min followed by a linear gradient of increasing acetonitrile to 40% and decreas-

ing methanol to 0% at 35–40 min, and a linear gradient at 40–60 min for returning the mobile phase to that at 0 min. The flow rate was 1.0 ml/min. Rutaecarpine and its oxidation metabolites were detected by measuring the absorbance at 344 nm.

For a scaled-up microsomal incubation, the final volume was 100 ml and reactions were performed in a 500 ml flask without cap in a water bath at 37 °C for 30 min with shaking. After incubation, the flask was placed in an ice-water bath and 5 ml 43% phosphoric acid was added to stop reaction. Oxidation products were extracted twice by 200 ml dichloromethane. The combined organic layer was dried using a rotor evaporator in a water bath at room temperature (Heidolph Instruments GmbH & Co KG, Alemania, Germany). Dried product was dissolved in acetonitrile and analyzed by a HPLC system equipped with an L-7100 pump and an L-7420 UV detector (Hitachi Ltd., Tokyo, Japan). Metabolites were separated using a C18 column (5C18-MS, 10 mm × 250 mm, Cosmosil, USA) and eluted by a mobile phase containing 26% acetonitrile, 10% methanol, and 0.04% phosphoric acid at a flow rate of 4.0 ml/min. Four metabolites were collected manually and extracted by two volumes of dichloromethane. The extracts were dried by a rotor evaporator and stored in freezer for ^{1}H NMR analysis.

2.4. Liquid chromatography–mass spectrometry (LC–MS)

The liquid chromatography system (ThermoQuest, San Jose, CA, USA) consisted of a degassing unit (SCM 1000), a quaternary pump (P 4000), an autosampler (AS 3000) with a 20 μl loop, and an UV detector (UV 2000). Separation of rutaecarpine oxidation metabolites and synthesized hydroxyrutaecarpines (1-, 2-, 3-, 4-, 9-, 10-, 11-, and 12-hydroxyrutaecarpine) was performed using a C_{18} reversed-phase column (Cosmosil 5C18-MS-II, 250 mm × 4.6 mm, 5 μm) at ambient temperature. A stepwise linear gradient elution of acetonitrile and water system was carried out as follows: 30% acetonitrile (0–60 min); 30–80% acetonitrile (60–80 min); 80% acetonitrile (80–100 min); 80–30% acetonitrile (100–105 min); 30% acetonitrile (105–120 min). The flow rate was 0.5 ml/min and absorbance at 344 nm was measured.

A Finnigan MAT LCQ ion trap mass spectrometer (ThermoQuest-Finnigan Co., San Jose, CA, USA) equipped with an electrospray ionization (ESI) source was used. The mass spectrometric data were acquired in the positive ion full-scan mode from *m*/*z* 150–1000 or selective ion monitoring mode (SIM) at *m*/*z* 304 [M + H$^+$] for metabolites and at *m*/*z* 288 for rutaecarpine. The conditions for ESI spectra were as follows: spray voltage, 4.5 kV; capillary voltage, 10 V; capillary temperature, 270 °C; sheath gas, 80 units; auxiliary gas, 20 units. Acquisition and processing of data from the mass spectrometer was performed using the Xcalibur software revision 1.0 (ThermoQuest-Finnigan Co., San Jose, CA, USA).

2.5. UV spectrometry and NMR spectroscopy

The spectral properties of rutaecarpine metabolites were analyzed within the wavelength range of 200–450 nm using a photodiode array detector G1315B (Agilent Technologies Inc., DE, USA) during HPLC analysis. The spectral properties of synthesized hydroxyrutaecarpine were analyzed within the wavelength range of 198–400 nm using a photodiode array detector L-7450A (Hitachi Ltd., Tokyo, Japan) during HPLC analysis. ^{1}H NMR spectra were recorded on a Varian Unity Inova-500 spectrometer (Varian Co., USA) at 499.887 MHz. The spectral width was set from −1 to 15 ppm (8000 Hz) and the digital resolution was 0.244 Hz. A switchable pulsed field gradient (PFG) probe was used for detection of proton nucleus. DMSO-d_6 was used as a solvent and the chemical shifts are reported in parts per million (δ) units relative to tetramethylsilane (TMS).

3. Results and discussion

In untreated rat liver microsomes, HPLC analyses of rutaecarpine oxidation products showed that the incubation of microsomes with rutaecarpine and a NADPH-generating system generated four main peaks of metabolites (M), which did not appear in the absence of the NADPH (Fig. 2). However, M3 and M4 were not well separated. Thus, in the LC–MS analysis, a linear gradient was used to separate M3 and M4 during the elution at 60–80 min (Fig. 3). The selective ion monitoring LC–MS chromatograms of oxidation products and synthetic standards are shown in Fig. 3A–C. The chromatograms are magnified to illustrate more clearly the profiles of metabolite peaks. Therefore, the rutaecarpine peak is over scale. 3-Methylcholanthrene-treatment highly increased the relative abundance of metabolite M1 as compared to untreated rats (Fig. 3B). This result suggested that CYP1A played a major

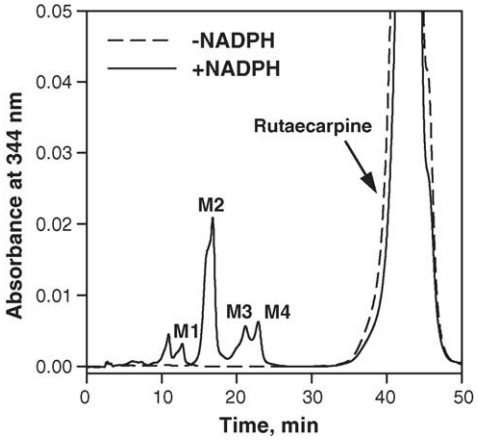

Fig. 2. HPLC chromatograms of rutaecarpine oxidation products of rat liver microsomes. Untreated rat liver microsomes were incubated with rutaecarpine in the absence and presence of a complete NADPH-generating system as described in Section 2.

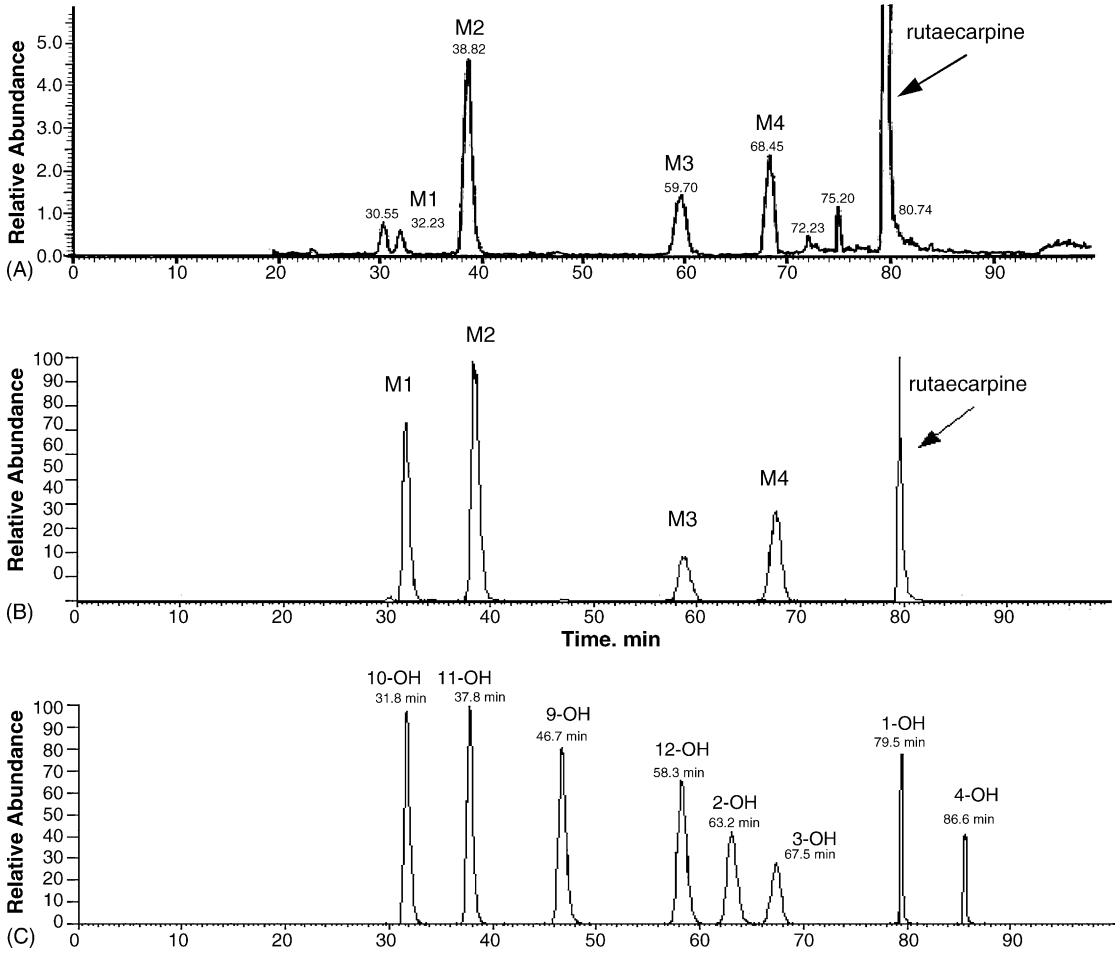

Fig. 3. Selective ion monitoring LC–MS chromatograms of rutaecarpine oxidation metabolites in untreated (A) and 3-methylcholanthrene-treated (B) rat liver microsomes. Rutaecarpine oxidation product from 1 ml incubation mixture of untreated rat liver microsomes was performed as described in Section 2. Oxidation products were dissolved in 0.5 ml acetonitrile and 20 μl was injected into HPLC for LC–MS analysis. The microsomal oxidation products of 3-methylcholanthrene-treated rats were prepared from the scaled-up incubation. (C) Selective ion monitoring LC–MS chromatogram of 1-, 2-, 3-, 4-, 9-, 10-, 11-, and 12-hydroxyrutaecarpine.

role in the formation of M1 metabolite. The mass spectra of these four metabolites were identical affording an $[M+H]^+$ ion at *m/z* 304. This result suggested the formation of monohydoxylated metabolites. Thus, 1-, 2-, 3-, 4-, 9-, 10-, 11-, and 12-hydroxyrutaecarpine were synthesized. LC–MS analysis showed that M1 (32.2 min), M2 (38.8 min), M3 (59.7 min), and M4 (68.5 min) had the same retention time of 10-, 11-, 12-, and 3-hydroxyrutaecarpine, respectively (Fig. 3C). The absorbance spectra of synthetic standards are shown in Fig. 4. M1–M4 (Fig. 4, left panel) had spectra similar to those of 10-,

Table 1
^{1}H NMR data of 10-, 11-, 12-, and 3-hydroxyrutaecarpine[a]

Position	10-Hydroxy-rutaecarpine	11-Hydroxy-rutaecarpine	12-Hydroxy-rutaecarpine	3-Hydroxy-rutaecarpine
1	7.65 (d, 8.0)	7.63 (d, 8.0)	7.68 (d, 8.0)	7.57 (d, 9.0)
2	7.79 (t, 8.0)	7.77 (t, 8.0)	7.82 (t, 8.0)	7.27 (dd, 9.0, 3.0)
3	7.45 (t, 8.0)	7.42 (t, 8.0)	7.48 (t, 8.0)	
4	8.14 (d, 8.0)	8.13 (d, 8.0)	8.16 (d, 8.0)	7.47 (d, 3.0)
7	4.42 (t, 7.0)	4.40 (t, 7.0)	4.44 (t, 7.0)	4.42 (t, 7.0)
8	3.08 (t, 7.0)	3.10 (t, 7.0)	3.15 (t, 7.0)	3.14 (t, 7.0)
9	6.88 (d, 2.0)	7.43 (d, 9.0)	7.11 (d, 8.0)	7.62 (d, 8.0)
10		6.62 (dd, 9.0, 2.0)	6.93 (t, 8.0)	7.07 (t, 8.0)
11	6.80 (dd, 8.5, 2.0)		6.67 (d, 8.0)	7.23 (t, 8.0)
12	7.28 (d, 8.5)	6.83 (d, 2.0)		7.45 (d, 8.0)
NH	11.6 (s)	11.4 (s)	11.3 (s)	11.8 (s)
OH	8.96 (s)	9.40 (s)		10.1 (s)

[a] δ (multiplicity, *J* in Hz) in ppm.

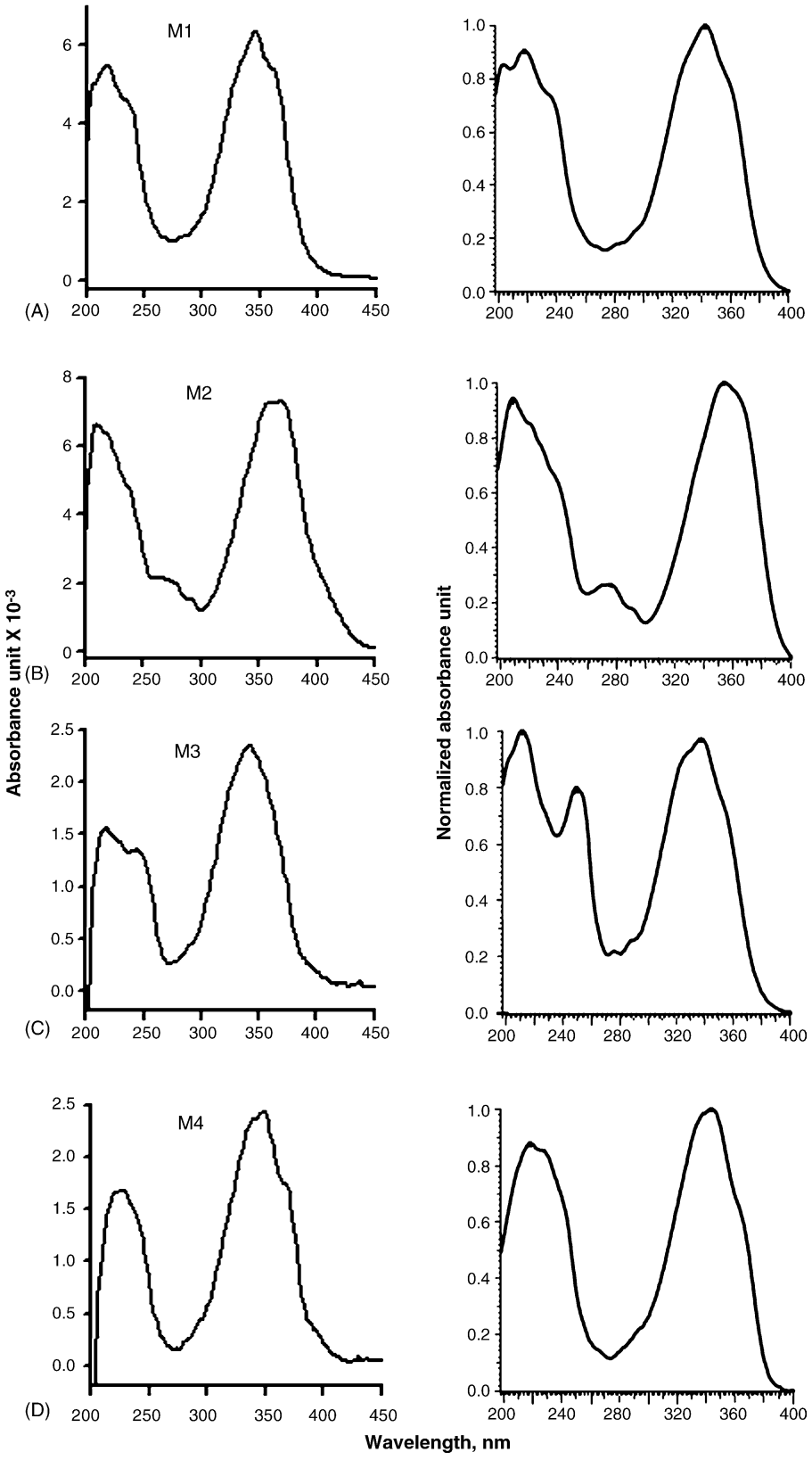

Fig. 4. The absorbance spectra of M1–M4 metabolites (left panel) and synthetic hydroxyrutaecarpines (right panel), 10- (A), 11- (B), 12- (C), and 3-hydroxyrutaecarpine (D). In (A)–(D), the relative absorbance intensity was normalized by the maximal absorbance.

11-, 12-, and 3-hydroxyrutaecarpine (Fig. 4, right panel), respectively. This result supported the structural identification that M1–M4 were 10-, 11-, 12-, and 3-hydroxyrutaecarpine, respectively. All of them had maximal absorbance around 340–354 nm. The detection of absorbance at 344 nm was suitable for rutaecarpine oxidation assay.

To further identify the structures of rutaecarpine oxidation metabolites, a scaled-up microsomal incubation was performed using liver microsomes of 3-methylcholanthrene-treated rats and four metabolites were separated by HPLC and isolated. Four metabolites were well separated using a semi-preparative column as described in Section 2 (Fig. 5A). The ^{1}H NMR data of 10-, 11-, 12-, and 3-hydroxyrutaecarpine are listed in Table 1. Our results showed that M1– M3 had chemical shifts with the same δ values as those of 10-hydroxyrutaecarpine, 11-hydroxyrutaecarpine, and 12-hydroxyrutaecarpine, respectively (Fig. 5B–G). The chemical shifts of the aromatic protons on A-ring (H-1–H-4) of M1–M3 were similar to those of rutaecarpine, respectively, which indicated the hydroxylation was occurred on E-ring of rutaecarpine. The ^{1}H NMR spectrum of 10-hydroxyrutaecarpine revealed an ABX pattern for aromatic protons on E-ring at δ 6.88 (H-9), 6.80 (H-11), and 7.28 (H-12), and the chemical shifts of H-9 and H-11 were shifted up-field due to hydroxy group on position 10, compared with the corresponding signals of rutaecarpine. The ^{1}H NMR spectrum of 11-hydroxyrutaecarpine also revealed a set of ABX aromatic protons on E-ring at δ 7.43 (H-9), 6.62 (H-10), and 6.83 (H-12), and the chemical shifts of H-10 and H-12 were shifted up-field due to hydroxy group on position 11. The ^{1}H NMR spectrum of 12-hydroxyrutaecarpine revealed consecutive aromatic protons on E-ring at δ 7.11 (H-9), 6.93 (H-10), and 6.67 (H-11), and the chemical shift of H-11 was shifted up-field due to *ortho* hydroxy group. The amount of M4 was small. However, no chemical shifts found at higher than 7.8 ppm indicated that the hydroxylation was occurred on A-ring of rutaecarpine, and several chemical shifts of M4 were detected at regions similar to those of 3-hydroxyrutaecarpine (Fig. 5H and I). The ^{1}H NMR spectrum of 3-hydroxyrutaecarpine revealed the chemical shifts of H-2 (δ 7.27) and H-4 (δ 7.47) were shifted up-field due to hydroxy group on position 3, compared with the corresponding signals of rutaecarpine. The results of liquid chromatograms and mass, absorbance, and ^{1}H NMR spectra demonstrated that M1–M4 were 10-, 11-, 12-, and 3-hydroxyrutaecarpine, respectively.

Using LC–tandem MS analysis, Lee et al. [3] reported that rutaecarpine was metabolized to form monohydroxylated and dihydroxylated metabolites by untreated rat liver microsomes. The hydroxylated positions were suggested to appear at A-, C-, and E-rings (Fig. 1). Our results demonstrated that monohydroxylated metabolites were the major metabolites and their structures are shown in Fig. 1. Our previous report showed that rutaecarpine fits well in the active site of human CYP1A2 [7]. The E-ring moiety of rutaecarpine approached to the heme moiety of CYP1A2 active site pocket. Consistent with the fitting results, 10-, 11-, and 12-hydroxyrutaecarpine were the main metabolites in untreated and 3-methylcholanthrene-treated rats. In the E-ring, the 9-position was the farthest site to the heme moiety. Our results showed that there was no 9-hydroxyrutaecarpine de-

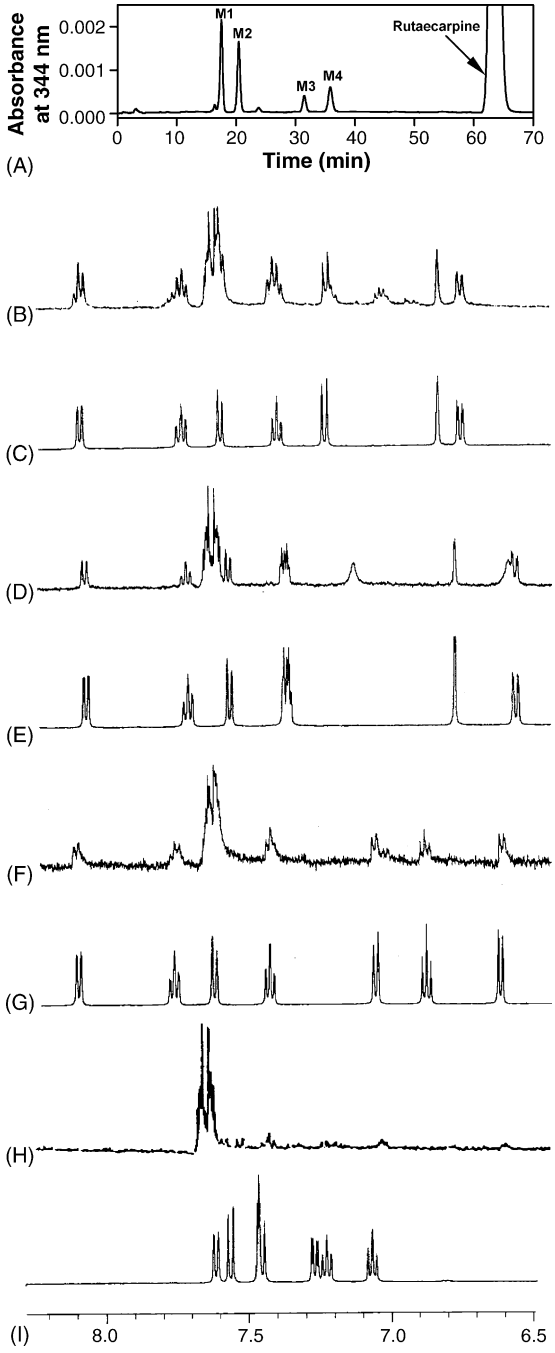

Fig. 5. (A) The HPLC chromatogram of a large-scale preparation of rutaecarpine oxidation products of 3-methylcholanthrene-treated rat liver microsomes. Oxidation products were separated by HPLC using a semi-preparative column as described in Section 2. (B)–(I) Partial ^{1}H NMR spectra (6.5–8.3 ppm) of microsomal rutaecarpine oxidation metabolites and synthetic hydroxyrutaecarpines: (B) M1; (C) 10-hydroxyrutaecarpine; (D) M2; (E) 11-hydroxyrutaecarpine; (F) M3; (G) 12-hydroxyrutaecarpine; (H) M4; and (I) 3-hydroxyrutaecarpine.

tected. According to our previous fitting results, A-ring was on the farthest sites to the heme moiety of human CYP1A2 [7]. However, 3-hydroxyrutaecarpine was identified in this report. The formation of 3-hydroxylated metabolite suggested that CYP forms other than CYP1A2 might be involved in rutaecarpine oxidation or rutaecarpine might bind to the active site of CYP1A2 in other ways. Lee et al. [12] reported that phenobarbital inducible CYP might also be involved in catalyzing rutaecarpine metabolism. The roles of CYP forms in rutaecarpine hydroxylation have been studied and will be discussed in our future publication.

In summary, our results demonstrated that rutaecarpine was oxidized by microsomal enzymes to form 3-, 10-, 11-, and 12-hydroxyrutaecarpine. In general, the xenobiotic hydroxylation metabolites have higher hydrophilicity than their parent compounds and show less biological activities or toxicities. For example, the metabolism of warfarin to form hydroxywarfarin greatly reduced its anticoagulant activity [13]. The potent hepatotoxin, aflatoxin B_1 is mainly detoxified by human liver microsomes to form the 3-hydroxylation metabolite, AFQ_1 [14]. However, safrole 1′-hydroxylation occupied the first step of carcinogenic activation of safrole [15]. For rutaecarpine hydroxylation metabolites identified in this report, there were no reports showing their biological activities. Thus, for a better clinical application, it is important to have further studies of the pharmacological and toxicological effects of rutaecarpine metabolites.

Acknowledgments

The authors thank Ms. Shu-Yun Wang for the preparation of rutaecarpine oxidation products of untreated and 3-methylcholanthrene-treated rat liver microsomes. This study was supported by grants NSC 92-2113-M-077-003 and NSC 91-2320-B077-010 from the National Science Council of the Republic of China.

References

[1] W. Tang, G. Eisenbrand, in: W. Tang, G. Eisenbrand (Eds.), Chinese Drugs of Plant Origin, Springer-Verlag, Berlin, 1992, p. 509.
[2] J.R. Sheu, Cardiovasc. Drug Rev. 17 (1999) 237.
[3] S.K. Lee, J. Lee, E.S. Lee, Y. Jahng, D.H. Kim, T.C. Jeong, Rapid Commun. Mass Spectrom. 18 (2004) 1073.
[4] F.P. Guengerich, in: P.R. Ortiz de Montellano (Ed.), Cytochrome P450, Plenum, New York, 1995, p. 473.
[5] Y.F. Ueng, J.J. Wang, L.C. Lin, S.S. Park, C.F. Chen, Life Sci. 70 (2001) 207.
[6] Y.F. Ueng, W.C. Jan, L.C. Lin, T.L. Chen, F.P. Guengerich, C.F. Chen, Drug Metab. Dispos. 30 (2002) 349.
[7] M.J. Don, D.F.V. Lewis, S.Y. Wang, M.W. Tsai, Y.F. Ueng, Bioorg. Med. Chem. Lett. 13 (2003) 2535.
[8] N. Iwata, K. Suzuki, K. Minegishi, T. Kawanishi, S. Hara, T. Endo, A. Takahashi, Eur. J. Pharmacol. 248 (1993) 243.
[9] J.P. Whitlock Jr., Ann. Rev. Pharmacol. Toxicol. 26 (1986) 333.
[10] F.L. Benten, T.E. Dillon, J. Am. Chem. Soc. 64 (1964) 1128.
[11] A.P. Alvares, G.J. Mannering, Mol. Pharmacol. 6 (1970) 206.
[12] S.K. Lee, N.H. Kim, J. Lee, D.H. Kim, E.S. Lee, H.G. Choi, H.W. Chang, Y. Jahng, T.C. Jeong, Planta Med. 70 (2004) 753.
[13] B.K. Park, Biochem. Pharmacol. 37 (1988) 19.
[14] F.P. Guengerich, W.W. Johnson, T. Shimada, Y.F. Ueng, H. Yamazaki, S. Langouët, Mutat. Res. 420 (1998) 121.
[15] J.L. Burkey, J.M. Sauer, C.A. McQueen, G. Sipes, Mutat. Res. 453 (2000) 25.